State Estimation and Feedforward Tremor Suppression for a Handheld Micromanipulator with a Kalman Filter

Brian C. Becker, *Student Member, IEEE*, Robert A. MacLachlan, *Member, IEEE*, Cameron N. Riviere, *Member, IEEE*

Abstract—**Active compensation of physiological tremor for handheld micromanipulators depends on fast control and actuation responses. Because of real-world latencies, real-time compensation is usually not completely effective at eliminating unwanted hand motion. By modeling tremor, more effective cancellation is possible by anticipating future hand motion. We propose a feedforward control strategy that utilizes tremor velocity from a state-estimating Kalman filter. We demonstrate that estimating hand motion in a feedforward controller overcomes real-world latencies in micromanipulator actuation. In hold-still tasks with a fully handheld micromanipulator, the proposed feedforward approach improves tremor rejection by over 50%.**

I. INTRODUCTION

MICROMANIPULATION during microsurgery and cell biological experiments requires precise, deft movements. For instance, new retinal operations include direct manipulation of vessels between 50-150 μm [1]. With physiological tremor amplitudes measured at over 100 μm [2], such micromanipulations are extremely difficult even for skilled surgeons. Advanced robotics technology such as the Johns Hopkins SteadyHand [3] aid surgeons by suppressing tremor with mechanical damping, providing a smoother, more accurate manipulation experience. Master/slave configurations such as the Robot Assisted MicroSurgery (RAMS) [4] or the robot-assisted vitreoretinal surgery system [5] depend on running tremor compensation filters between the haptic input and the output tip. Micron, the micromanipulator built in our lab, is a fully handheld micromanipulator with actuators between the handle and the tip of the instrument [6]. By offsetting the tip relative to the handle, Micron is able to compensate for a surgeon's tremor [7].

A handheld micromanipulator such as Micron has a number of advantages. First, it is small and lightweight, making it easy-to-use and inexpensive. Second, handheld instruments are intimately familiar to surgeons, so Micron can leverage surgeons' experience and skills with little training. Third, small handheld instruments offer greater

B. C. Becker, R. A. MacLachlan, and C. N. Riviere are with the Robotics Institute, Carnegie Mellon University, Pittsburgh, PA 15213 USA (e-mail: camr@ri.cmu.edu).

safety because the surgeon can more easily override or remove the instrument in cases of malfunction. Finally, if the equipment stops working, the surgeon can simply switch Micron off and use it as a normal handheld instrument.

However, handheld micromanipulators pose additional challenges over purely mechanical damping or master/slave configurations. Because the handle and tip are mechanically coupled, the actuator between them must operate at very high control frequencies. If the actuator responsible for moving the tip relative to the handle cannot react fast enough to counter hand motion, tremor compensation and other micromanipulation tasks become degraded. Since real-world systems exhibit some latency, a pure feedback control system without sufficient bandwidth will result in imperfect compensation of tremor, as evidenced in reported residual errors of 10-60 μm during hold-still tasks [8]. This error must be viewed in the context of retinal surgery, where membranes in the eye are only tens of microns thick, and tearing them can permanently damage eyesight.

To address actuator latency in handheld micromanipulators such as Micron, we propose to integrate a Kalman filter with feedforward control for increased suppression of tremor. Section II describes background material, including the Kalman filter and the Micron manipulator. In Section III, we present our Kalman filter formulation and feedforward control system. We demonstrate in Section IV the improved results of the proposed feedback+feedforward control system and conclude in Section V with a discussion of the results and areas of future work.

II. BACKGROUND

In a handheld micromanipulator, we assume there is some set point $p^s \in \mathbb{R}^3$ that is selected as the goal position for the tip of the micromanipulator. While the focus of this paper is

Fig. 1. Micron micromanipulator without casing to illustrate the piezoelectric motors between the handle and tip of the instrument, which enable the tip to actuate independently of the handle (hand) motion.

not on how to best select the set point, it can be generated by a tremor-compensation filter [7], virtual fixtures [8], or other behaviors [9, 10]. Once the set point has been generated by a higher-level control system, the low-level control system attempts to track the set point with the tip of instrument.

Disturbances to the tip arise from a variety of sources including vibrations, resonances, or contact with tissue. However, the largest disturbance in a micromanipulator system is generally hand motion, which includes both voluntary movement and involuntary tremor. Typically, tremor is treated as the disturbance, but voluntary motion can be thought of as a disturbance too, such as the case when the set point is being generated from virtual fixtures or motion scaling. For the purposes of this paper, we consider all hand motion that does not coincide with the set point motion to be a disturbance to the control system.

A. Feedforward Control

In feedback systems, disturbances are handled as they cause the output to drift away from the set point; this error is then fed back into the control system to bring the output back to the set point. One popular feedback control approach is PID (Proportional, Integral, and Derivative) gains on the error. However, feedback control can only react to disturbances after they have so affected the system state that the deviation from the goal is noticeable. This error is then exacerbated by latencies in actuation as it may take several cycles before the actuators respond to eliminate the error.

If the disturbance is predictable or correlated with some other predictable variable (e.g. gravity, friction), feedforward control can couple the set point directly to the control variable. By modeling the disturbance and its effect on the system, control effort can be applied before error occurs. To compensate for latencies in the actuation, short-term future predictions from the model can be used to drive the actuators in anticipation of how the disturbance will affect the system. When suppressing tremor in a handheld micromanipulator, the hand motion that does not correspond to the set-point motion is the disturbance. Such feedforward rejection of tremor requires good estimation of both observed and unobserved motion states of the system.

B. Kalman Filter

Optimal estimation of the current state of a system is a wide field [11], but one of the most popular state estimators is the Kalman filter [12, 13]. A main assumption of the Kalman filter is that observations, or sensor readings, z of a system follow some dynamics. The current state of the system $x \in \mathbb{R}^n$ is the n minimum number of variables necessary to predict future behavior of the system. If the system is linear, states evolve according to the dynamic model A of the system and with the inputs u to the system (i.e., actuation). More formally, we can represent the state transitions discretely at time step k as:

$$x_k = A_k x_{k-1} + B_k u_k \tag{1}$$

$$y_k = C_k x_k \tag{2}$$

where B_k and C_k describe the impact of inputs u on the state x and how observations y are made from the current state x, respectively. Assuming Gaussian noise on the observations z and the dynamic model A characterized by covariances R and Q, respectively, the Kalman filter optimally estimates the system's state x at each time step:

$$\hat{x}_k = A_k x_{k-1} + B_k u_k \tag{3}$$

$$\hat{P}_k = A_k P_{k-1} A^T + Q_k \tag{4}$$

$$\hat{y}_k = z_k - H_k \hat{x}_k \tag{5}$$

$$S_k = H_k \hat{P}_k + R_k \tag{6}$$

$$K_k = \hat{P}_k H^T S_k^{-1} \tag{7}$$

$$x_k = \hat{x}_k + K_k y_k \tag{8}$$

$$P_k = (I - K_k H_k) \hat{P}_k \tag{9}$$

where (3-4) are known as the predict step, which use the dynamic model and inputs to the system to predict the state $\hat{x}$ at the next time step. Equations (5-9) are known as the update steps, where the residual between the predicted state $\hat{x}$ and the measured state z is used to calculate the Kalman gain K, which optimally mixes between the measurements and the dynamic model to yield the best estimate of the current state x. P is the error covariance that represents the accuracy of the state estimate x. The Kalman filter has been widely successful in a number of different applications.

C. Micron Micromanipulator

Micron (Figure 1) is a 3 degree of freedom (DOF), fully handheld micromanipulator [6, 7] with three piezoelectric actuators mechanically coupling the tip and handle of the instrument. By actuating these motors, the instrument tip is able to move with respect to the handle in a 2x2x1 mm range of motion to cancel tremor, snap to virtual fixtures [8], apply grids of laser burns [9], or perform other intelligent behaviors [10]. High-rate positioning information is achieved with low-latency optical tracking hardware named ASAP [14]. Using three pulsed LEDs on the tip of the instrument and one on the handle, two Position Sensitive Detectors (PSDs) at a 60° angle triangulate the frequency-modulated LEDs at 2 kHz for full 6 DOF positioning of the tip and handle with <10 μm RMS error. Micron is operated under a surgical microscope equipped with cameras for vision-based surgical control and post-procedure evaluation (see Figure 2).

III. METHODS

By using a Kalman filter for state estimation of both the handle and tip, we propose a feedforward control strategy that anticipates hand motion to more effectively suppress
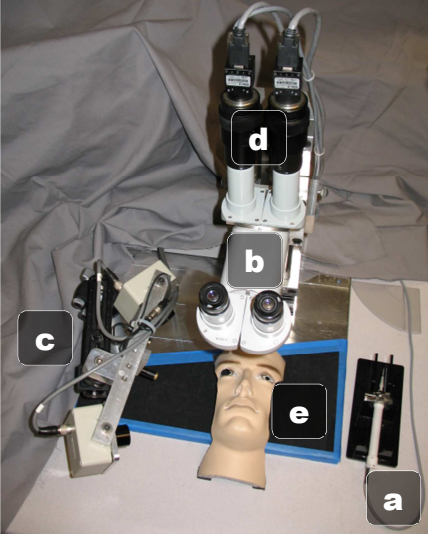
Fig. 2. Experimental setup: (a) Micron (b) Operating microscope (c) ASAP optical trackers (d) Stereo cameras (e) Eye/face phantom.

tremor in handheld micromanipulators.

A. State Estimation with Kalman Filter

Full 6-DOF pose information for the tip and handle is calculated from the LEDs via triangulation and the application of the closed-form Horn calculation [15] on the recovered 3D positions of the LEDs. Because the raw 2 kHz pose data is noisy and numerically calculating velocity or acceleration data would be extremely noisy, we use a Kalman filter [12, 13] for complete state estimation of the pose of Micron's tip and handle position. We choose a linear Kalman filter similar to [16] since the sample rate is sufficiently high to well approximate the nonlinearities in the system. Furthermore, recent work has shown that nonlinear versions such as the Extended or Unscented Kalman filters have difficulties modeling tremor with nonlinear harmonic models [17]. Because the hand motion contains low-frequency voluntary movement (<1 Hz) combined with involuntary tremor motions (10-20 Hz), we use a constant acceleration motion represented by the state transition:

$$\begin{bmatrix} p \\ \dot{p} \\ \ddot{p} \end{bmatrix}_k = \begin{bmatrix} 1 & dt & \frac{1}{2}dt^2 \\ 0 & 1 & dt \\ 0 & 0 & 1 \end{bmatrix} \begin{bmatrix} p \\ \dot{p} \\ \ddot{p} \end{bmatrix}_{k-1} \tag{10}$$

with $P = [p, \dot{p}, \ddot{p}]^T$ representing the position, velocity, and acceleration of the system.

To represent orientation, we investigated quaternions but used Euler angles instead for the following reasons. First, Micron's orientation only changes slightly during operations, usually by only 10-20°, so gimbal lock is not an issue. Second, Euler angles' representation with three variables instead of quaternion's overrepresented four variables leads to easier calculations, as issues of heteroscedasticity and re-normalization do not arise. More importantly, since the Kalman filter must be run at 2 kHz in a real-time operating system, using three variable

representations for orientation results in faster calculations, especially in the slow inverse calculation of (7). Third, quantitative analysis revealed that in typical usage scenarios, the difference between estimations using Euler angle representations and those using quaternions is negligible. We use the constant angular velocity model for the orientation:

$$\begin{bmatrix} \theta \\ \dot{\theta} \end{bmatrix}_k = \begin{bmatrix} 1 & dt \\ 0 & 1 \end{bmatrix} \begin{bmatrix} \theta \\ \dot{\theta} \end{bmatrix}_{k-1} \tag{11}$$

with $\Theta = [\theta, \dot{\theta}]^T$ representing the orientation angle and angular velocity in the world frame. Denoting the state transitions of position and orientation as A^p and A^o and the full 15 state vector $x = [P_X, P_Y, P_X, \Theta_Z, \Theta_Y, \Theta_Z]$, we can build the full 6-DOF state transition in block-diagonal form:

$$\begin{bmatrix} P_X \\ P_Y \\ P_Z \\ \Theta_X \\ \Theta_Y \\ \Theta_Z \end{bmatrix}_k = \begin{bmatrix} A_X^p & \mathbf{0_3} & \mathbf{0_3} & & & \\ \mathbf{0_3} & A_Y^p & \mathbf{0_3} & & \mathbf{0_{9\times6}} & \\ \mathbf{0_3} & \mathbf{0_3} & A_Z^p & & & \\ & & & A_X^o & \mathbf{0_2} & \mathbf{0_2} \\ & \mathbf{0_{6\times9}} & & \mathbf{0_2} & A_Y^o & \mathbf{0_2} \\ & & & \mathbf{0_2} & \mathbf{0_2} & A_Z^o \end{bmatrix} \begin{bmatrix} P_X \\ P_Y \\ P_Z \\ \Theta_X \\ \Theta_Y \\ \Theta_Z \end{bmatrix}_{k-1} \tag{12}$$

Measurements at each time-step are represented as $z = [p_X, p_y, p_z, \theta_X, \theta_Y, \theta_Z]$. Measurement and process covariances are set to $R = [10^3, 10^3, 10^2, 10^3, 10^3, 10^2] * I_{6\times6}$ and $Q = 10^{-1} * I_{15\times15}$, respectively. Because the tip and handle are only loosely coupled, separate Kalman filters are used for state estimation of the tip and handle to reduce computational requirements. For the handle, no hand actuation input is available, so control input $u_k = 0$. For the tip Kalman filter, the forward kinematics J and model B of the actuators are calculated once from a ~30s calibration procedure. Because the actuators are in the body frame while all other state variables are in the world frame, the actuator input u_k is first rotated into the world frame by the current orientation R_k estimated from the state $[\theta_{X,k}, \theta_{Y,k}, \theta_{Z,k}]^T$:

$$\hat{x}_k = Ax_{k-1} + BR_k u_k \tag{13}$$

giving us a prediction model that takes into account both the internal dynamics of the system and any actuation.

By integrating system dynamics, actuator models, and measurements, the Kalman filter estimates of the position, velocity, acceleration, orientation, and angular velocity of both the tip and handle of Micron.

B. Feedforward Control

During handheld operation, unwanted movement of the hand causes the tip p^t to deviate from the set-point goal p^s. Inverse kinematics J^{-1} translate measured error $e = p^s - p^t$ into corrective actuation with a PID controller, generating feedback control u_{FB}:

$$u_{FB} = K_P J^{-1} e + K_I \int J^{-1} e + K_D \frac{d}{dt} J^{-1} e \tag{14}$$

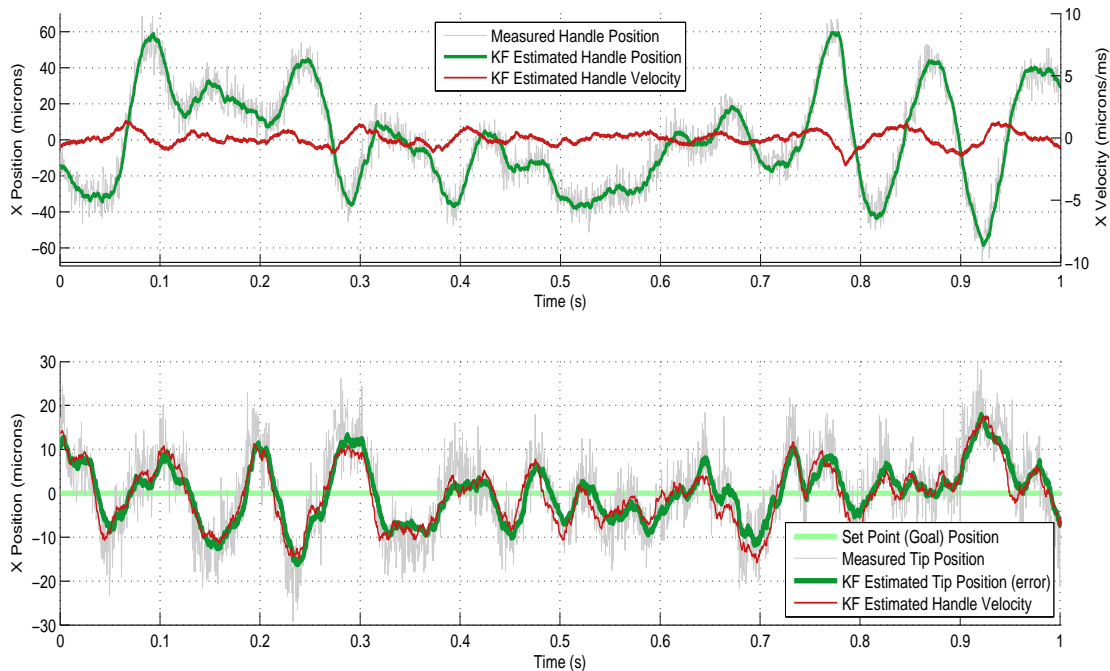where K_P, K_I, and K_D are the proportional, integral, and

Fig. 3. (Top) State estimation of hand motion by Kalman Filter compared to raw measurements. (Bottom) Kalman filter estimates of Micron's tip position during a hold-still task with feedback control. Notice the good agreement between the hand velocity and the error seen at the tip position.

derivative gains.

Since the tip of Micron is mechanically tied to the handle via actuators, we use a straightforward process model that assumes the tip velocity $\dot{p}^t$ is composed of the handle velocity $\dot{p}^h$ plus the control effort of the actuators u_{FB}:

$$\dot{p}^t = \dot{p}^h + u_{FB} \quad (15)$$

From (15), we see the resulting error e in the output tip after feedback control is proportional to the rate of change of the hand position, or $\dot{p}^h$. Intuitively, the tip velocity should match the set-point velocity $\dot{p}^s$, giving us a feedforward error term e_{FF}:

$$e_{FF} = \dot{p}^h - \dot{p}^s \quad (16)$$

Assuming the set-point velocity is negligible ($\dot{p}^h \gg \dot{p}^s$), our error e_{FF} reduces to hand velocity $\dot{p}^h$ and feedforward control u_{FF} can be integrated into the system with a PID controller similar to (14):

$$u_{FF} = K_P J^{-1} \dot{p}^h + K_I \int J^{-1} \dot{p}^h + K_D \frac{d}{dt} \dot{p}^h \quad (17)$$

Both feedback and feedforward inputs are applied at each time step, with the aggressiveness of the feedforward control inputs defined by λ:

$$u = u_{FB} + \lambda u_{FF} \quad (18)$$

Thus, to more robustly maintain a set point, hand movements estimated by the Kalman filter can be anticipated as they occur instead of after causing error.

IV. RESULTS

In this section, we present results of the Kalman filter state estimation of Micron and its effect on tremor suppression. Using the state-estimation to anticipate tremor, we use implement and test feedforward control in hold-still tasks with Micron, our handheld micromanipulator.

A. State Estimation

Figure 3 shows the Kalman filter state estimation of the handle position and velocity for a one second time slice of the X axis. The Kalman filter is able to accurately and smoothly estimate not only position, but higher order derivatives while ignoring significant amounts of sensor noise. Also shown is the agreement between the tip error under PID feedback-only control and the velocity, which experimentally validates (16). The Y and Z axis graphs are similar to the figures shown for the X axis.

B. Experimental Protocol

Tests were performed with Micron under a board-approved protocol to evaluate the Kalman filter state estimation and the tremor suppression effects of the feedback+feedforward controller. All experiments were performed with a single individual familiar with Micron but without surgical experience. The task of interest is hold-still, in which the operator attempts to hold the tip motionless at a fixed 3D set point. Visual cues are presented to the operator on a 3D monitor to help the operator avoid drifting too far from the set point, which would saturate the actuators. To alleviate operator bias, controllers are executed at random in 5 s intervals without notifying the operator.
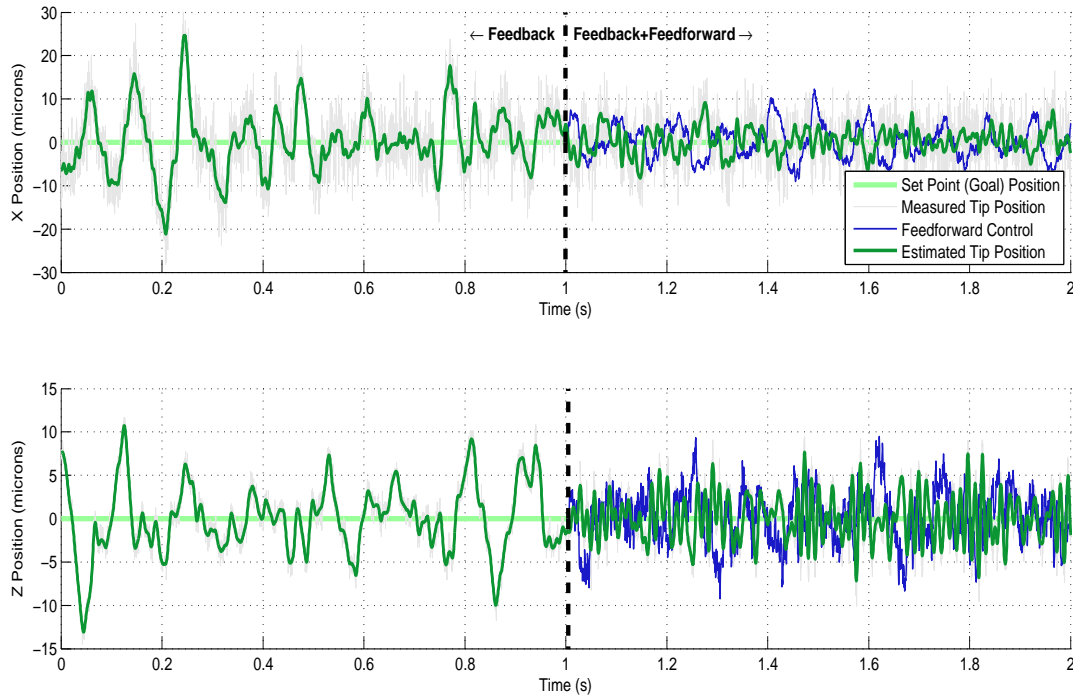
Fig. 4. Comparison of the feedback vs. feedback+feedforward controller for tremor suppression (top: transverse, bottom: axial). The controller is swapped out dynamically at $= 1\,s$. Although tremor suppression is not completely effective in either case, the addition of the feedforward component is clearly beneficial.

Ground truth for the tip position is constructed by low-passing the tip position with a 100 Hz bi-directional, zero-lag 2nd order Butterworth filter. Because manipulator resonances begin around 100 Hz, this serves as a reasonable ground truth. Furthermore, the zero-lag low-pass filter is a more unbiased estimator of the ground truth than the Kalman filter because the system feeds the output of the Kalman filter back into the control system. Combined with the actuator model, this could introduce biases into the estimation. Each controller is evaluated by calculating RMS error between the ground truth tip position and the set point goal.

C. Feedforward Tremor Suppression

When feedforward control with Kalman filter estimation is added to the feedback controller, more tremor is suppressed. Figure 4 demonstrates the additional suppression by showing the activation of the feedback+feedforward controller during a hold still task. Because of imperfect estimation, actuation latencies, and other nonlinearities, perfect cancellation is not achieved; however, tremor-caused disturbances of 10-20 μm magnitudes can generally be reduced to 5-10 μm with the feedforward approach. Table I lists the feedback+feedforward controller as reducing the RMS error by 56.7% as compared to only using the feedback controller. Figure 5 shows a power spectrum of the error for each controller. The feedback+feedforward controller performs better at low frequencies, and peaks somewhat around 60 Hz. However, this is not a concern, as very little energy exists at this frequency. As a best case bound for

handheld tremor suppression, we present the results of Micron maintaining a set point in the absence of any hand motion and tremor; this is achieved by clamping the handle with rubber in a vise.

The closed-loop frequency response of the new feedback+feedforward controller compared to the baseline controller is shown in Figure 6. A sine wave chirp signal sweeping 1 Hz to 1 kHz is injected into the pose of the instrument during handheld operation. The tip position response to the injected stimulus is recorded over many runs to average out handheld motion. Notice the feedback+feedforward controller does significantly better
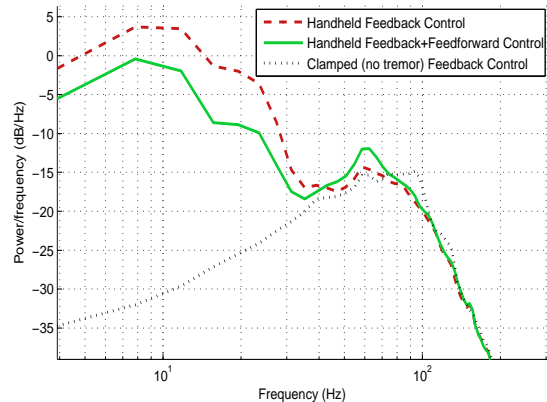

Fig. 5. Power spectrum of the two controllers under handheld conditions: the baseline controller and the feedforward controller. For comparison to a tremor-free case, the baseline feedback controller operating in a clamped rubber vise is shown also.

TABLE I
ERROR OF CONTROLLERS

Method	RMS Error (μm)	Improvement Over Baseline (%)
Baseline Feedback	7.9	-
Clamped (No Tremor)	1.4	-
Feedback+Feedforward	3.4	56.7

Mean performance measured with Root Mean Square (RMS) of the error signal represented as percent improvement over the baseline feedback-only controller. Best attainable tremor suppression should be approximated by the case where Micron is clamped in a vise (i.e. no tremor).
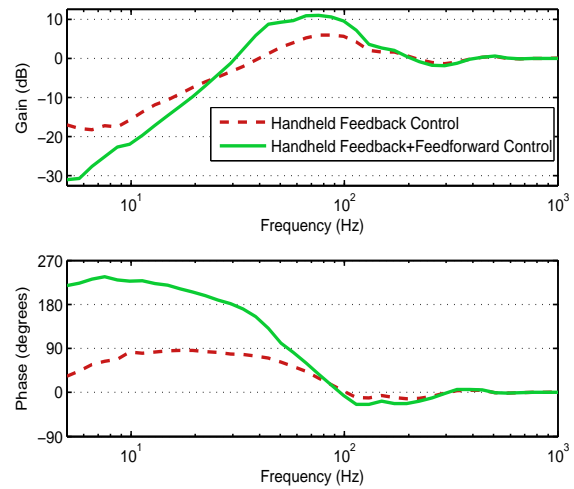

Fig. 6. Frequency response of the two controllers under handheld conditions: the baseline feedback controller and the feedback+feedforward controller. Notice the additional attenuation of error at low frequencies in the 5-20 Hz tremor range. This frequency response is for the transverse axis of the manipulator; the lateral response is similar.

than the the feedback-only controller in the lower frequencies where tremor is most strongly exhibited. At 10 Hz, where peak tremor power occurs, the attenuation in the response is -7 dB. By the Bode Integral Theorem, we expect to see an increase in the response at higher frequencies corresponding to the decrease at lower frequencies, which we do. However, as evidenced in the power spectrum in Figure 5, there is significantly less energy in the system at these higher frequencies so overall the system demonstrates a net gain in tremor compensation.

V. DISCUSSION

We have demonstrated that applying a Kalman filter for state estimation of hand motion in a feedforward controller can produce superior tremor suppression. A Kalman filter for both the tip and the handle of Micron is run at 2 kHz to fully estimate the position, velocity, acceleration, orientation, and angular velocities. By modeling the effect of physiological tremor on the process plant, feedforward control uses estimated handle velocity to anticipate and reject extraneous hand motions. Experiments show a reduction in RMS error of more than half, which corresponds to approximately -7 dB rejection ratio. This significantly improves accuracy around tiny anatomy such as retinal vessels and reduces trauma to surrounding tissue caused by tremor. In the future, we plan on analyzing lower-level current control on the piezoelectric motors, examining vibration estimations of the sensors, and incorporating tremor prediction algorithms [18-20].

REFERENCES

[1] L. A. Bynoe, R. K. Hutchins, H. S. Lazarus, and M. A. Friedberg, "Retinal endovascular surgery for central retinal vein occlusion: initial experience of four surgeons," *Retina,* vol. 25, pp. 625-32, 2005.

[2] S. P. N. Singh and C. N. Riviere, "Physiological tremor amplitude during retinal microsurgery," in *Proc. Conf. Proc. IEEE Eng. Med. Biol. Soc.*, 2002, pp. 171-172.

[3] B. Mitchell, J. Koo, M. Iordachita, P. Kazanzides, A. Kapoor, J. Handa, G. Hager, and R. Taylor, "Development and application of a new steady-hand manipulator for retinal surgery," in *Proc. IEEE Int. Conf. Robot. Autom.*, 2007, pp. 623-629.

[4] H. Das, H. Zak, J. Johnson, J. Crouch, and D. Frambach, "Evaluation of a telerobotic system to assist surgeons in microsurgery," *Computer Aided Surgery,* vol. 4, pp. 15-25, 1999.

[5] T. Ueta, Y. Yamaguchi, Y. Shirakawa, T. Nakano, R. Ideta, Y. Noda, A. Morita, R. Mochizuki, N. Sugita, and M. Mitsuishi, "Robot-Assisted Vitreoretinal Surgery:: Development of a Prototype and Feasibility Studies in an Animal Model," *Ophthalmology,* vol. 116, pp. 1538-1543, 2009.

[6] R. A. MacLachlan, B. C. Becker, J. C. Tabares, G. W. Podnar, J. Louis A. Lobes, and C. N. Riviere, "Micron: an Actively Stabalized Handheld Tool for Microsurgery," *IEEE Trans. Robot.,* submitted.

[7] J. Cuevas Tabarés, R. A. MacLachlan, C. A. Ettensohn, and C. N. Riviere, "Cell Micromanipulation with an Active Handheld Micromanipulator," in *Conf. Proc. IEEE Eng. Med. Biol. Soc.*, 2010, pp. 4363-4366.

[8] B. C. Becker, R. A. MacLachlan, G. D. Hager, and C. N. Riviere, "Handheld Micromanipulation with Vision-Based Virtual Fixtures," in *Proc. IEEE Int. Conf. Robot. Autom.*, 2011.

[9] B. Becker, R. MacLachlan, L. Lobes Jr, and C. Riviere, "Semiautomated intraocular laser surgery using handheld instruments," *Lasers Sur. Med.,* vol. 42, pp. 264-273, 2010.

[10] B. C. Becker, S. Voros, J. Louis A. Lobes, J. T. Handa, G. D. Hager, and C. N. Riviere, "Retinal vessel cannulation with an image-guided handheld robot," in *Conf. Proc. IEEE Eng. Med. Biol. Soc.*, 2010, pp. 5420-5423.

[11] D. Simon, *Optimal state estimation: Kalman, H [infinity] and nonlinear approaches*: John Wiley and Sons, 2006.

[12] R. E. Kalman, "A new approach to linear filtering and prediction problems," *J. of Bas. Engr.,* vol. 82, pp. 35-45, 1960.

[13] G. Welch and G. Bishop, "An introduction to the Kalman filter," University of North Carolina, Chapel Hill, NC1995.

[14] R. A. MacLachlan and C. N. Riviere, "High-speed microscale optical tracking using digital frequency-domain multiplexing," *IEEE Trans. Instrum. Meas.,* vol. 58, pp. 1991-2001, 2009.

[15] B. Horn, "Closed-form solution of absolute orientation using unit quaternions," *J. Opt. Soc. of Am. A,* vol. 4, pp. 629-642, 1987.

[16] K. Dorfmüller-Ulhaas, "Robust optical user motion tracking using a Kalman filter," in *Proc. ACM Symp. on Virt. Real. Soft. Tech.*, 2003.

[17] A. Bo, P. Poignet, F. Widjaja, and W. Ang, "Online pathological tremor characterization using extended Kalman filtering," in *Conf. Proc. IEEE Eng. Med. Biol. Soc.*, 2008, pp. 1753-1756.

[18] C. N. Riviere, W. T. Ang, and P. K. Khosla, "Toward active tremor canceling in handheld microsurgical instruments," *IEEE Trans. Robot. Autom. ,* vol. 19, pp. 793-800, 2003.

[19] K. Veluvolu, W. Latt, and W. Ang, "Double adaptive bandlimited multiple Fourier linear combiner for real-time estimation/filtering of physiological tremor," *J of Bio. Sig. Proc. Con.,* vol. 5, pp. 37-44, 2010.

[20] J. Timmer, "Modeling noisy time series: physiological tremor," *Intl. J. Bifurcation and Chaos,* vol. 8, pp. 1505-1516, 1998.